A STUDY OF THE DYNAMICS OF DUAL-PARTICLES SETTLING CLOSE TO A VERTICAL WALL

Lisa T. Prahl
Division of Fluid Mechanics
Lund Institute of Technology
P.O. Box 118, S-221 00 Lund, Sweden
Lisa.Prahl@vok.lth.se

Johan Revstedt and Laszlo Fuchs
Division of Fluid Mechanics
Lund Institute of Technology
P.O. Box 118, S-221 00 Lund, Sweden
Johan.Revstedt@vok.lth.se, Laszlo.Fuchs@vok.lth.se

ABSTRACT

Simulations of single and multiple spherical particles settling under gravity in the presence of a vertical wall are performed. In this study, the Reynolds number based on a characteristic velocity set to unity and the diameter of the sphere is varied in the range from 1 to 1000 and the density ratio in the range from 1.5 to 8. Interaction between particles as well as with the wall is investigated. The particles are modeled by using the Volume of Solid (VOS) approach, a method based on the Volume of Fluid (VOF) approach.

The simulations showed that the motion of both single and dual spheres falling side by side is affected by the wall. Also, a dominant frequency for the oscillatory movements perpendicular to the wall was detected.

INTRODUCTION

For a wide range of applications, both industrial and environmental, it is of interest to be able to accurately predict the transport of particles to improve the understanding of particle dynamics. In order to achieve this, it is therefore important to have good models for the transport of the particulate phase, including the interaction between particles as well as with solid boundaries.

The stability of the flow past spheres as well as the wake formation behind spheres has thoroughly been investigated in previous studies, mostly for single sphere cases. For multiple sphere arrangements; side-by-side and tandem arrangements have been the most frequently investigated formations (Kim et. al (1993), Liang et. al (1996), Olsson & Fuchs (1998), Chen & Wu (2000), Zhu et. al (2001), Tsuji et. al (2003)). These studies all conclude that the distance between spheres plays an important roll on the drag force for spheres held fixed in a uniform flow. In general, when two identical spheres are held fixed in a side-by-side arrangement, the drag force increases with a decreasing separation distance between the spheres and with increasing Reynolds number. Also, at very small separation distances, with the spheres almost in contact, the spheres can from a flow point of view be considered as a single body (Olsson & Fuchs (1998), Folkersma *et al.* (2000)). For a tandem arrangement, small separation distances leads to decreased drag forces. As the spheres are moved apart, the drag force gradually levels off to the value of an isolated spherical particle (Liang *et al.* (1996), Olsson & Fuchs (1998)).

The two parameters that experimentally have been observed to influence the dynamics of the motion of a solid sphere falling under gravity are the Reynolds number and the particle density. Solid spheres settling due to gravity were studied by Mordant & Pinton (2000). Their results showed that at Reynolds numbers close to the onset of vortex shedding, approximately 400, the particles with lower density showed velocity oscillations, implying that the velocity is no longer a monotonous function of time.

In studies carried out by Jayaweera & Manson (1964) and Wu & Manasseh (1998), the behaviour of dual particles falling under gravity was experimentally investigated. In both studies it was concluded that dual particles settle faster than a single particle for lower Reynolds numbers. However, Wu & Manasseh (1998) reported that due to particle separation, this is no longer valid as the Reynolds number is increased. When two spherical particles are released in a side-by-side arrangement, each sphere will rotate inwards and the particles will separate until a final separation distance is reached. The rate of rotation is amplified with increasing Reynolds number, enhancing the separation distance, which in turn causes the rotational rate to decrease. Also, as the fluid-particle density ratio is increased, so is the particle separation distance. However, it should be mentioned that for $Re < 0.1$, no particle separation has been reported to occur. For a tandem particle case with two equally sized spheres, the rear particle is accelerated into the wake of the leading particle, rotates around and places itself in the same horizontal plane as the leading particle and, finally, the spheres separates from each other in a similar way as in the side-by-side arrangement. Considering a case with a smaller trailing particle, the sphere will roll around the leading larger sphere instead of rotating around it, observed by Jayaweera & Manson (1964) and Zhao & Davis (2001).

The purpose of this work is to study single and dual spherical particles settling under gravity. The focus is on investigating how the motion of falling spheres is affected by the presence of a vertical plane wall. Validation is performed for Stokes flow around a sphere. Both single and a dual sphere formation are considered; spheres falling side by side. These results include cases with different density ratios and Reynolds numbers, and, for the dual-sphere cases, the space between the two particles is taken as a free parameter.

NUMERICAL METHOD

The governing equations of mass and momentum for an unsteady, viscous, incompressible Newtonian fluid may be expressed as;

$$\frac{\partial u_j}{\partial x_j} = 0 \tag{1}$$

$$\frac{\partial u_i}{\partial t} + u_j \frac{\partial u_i}{\partial x_j} = -\frac{\partial p}{\partial x_i} + \frac{1}{Re}\frac{\partial}{\partial x_j}\frac{\partial u_i}{\partial x_j} \tag{2}$$

Equations (1) and (2) are discretized on a Cartesian staggered grid using second order central differences for all spatial derivatives except for the convective terms where a first order upwind scheme is used. A defect correction is used to improve the accuracy of the spatial discretizations of the momentum equations without loss of numerical stability to third order for convective terms and to forth order to the remaining terms. A multi-grid method is used to iteratively solve the system of equations in each time step to improve the convergence rate of the solution.

Volume of Solid (VOS)

The Volume of Solid (VOS) method (Lörstad & Fuchs, 2001) is used to represent the spherical particles. VOS is based on the Volume of Fluid (VOF) method. However, in VOS, the "second fluid" is a solid body that is assumed to have an infinite viscosity. With the shear stresses being nearly constant due to the fact that viscous forces at dominating close to the surface and the assumed infinite viscosity of the solid phase, the averaged viscosity can be represented by the following equation;

$$\mu = \mu_1 / \alpha \tag{3}$$

α being the phase variable representing the amount of fluid in each cell, $0 \leq \alpha \leq 1$. Since there is no flow inside the solid body ($\alpha = 0$), cells containing the solid phase will be blocked and no computations will be carried out for these cells. With a constant density, equation (3) can be written as;

$$\nu = \nu_1 / \alpha \tag{4}$$

Using the relation above, the viscosity ratio term, $\delta\nu$ can be defined as;

$$\delta\nu = \frac{\nu}{\nu_1} = \frac{1}{\alpha} \tag{5}$$

It should be noted that in most computational cells, the viscosity ratio will have the value of unity. With the definition of the viscosity ratio, $\delta\nu$, as stated in equation (5), the continuity and momentum equations governing an isothermal, incompressible flow of a Newtonian fluid are as follows;

$$\frac{\partial u_i}{\partial x_i} = 0 \tag{6}$$

$$\frac{\partial u_i}{\partial t} + u_j \frac{\partial u_i}{\partial x_j} = -\frac{\partial p}{\partial x_i} + \frac{1}{Re}\frac{\partial}{\partial x_j}\left(\delta\nu \frac{\partial u_i}{\partial x_j}\right) \tag{7}$$

By integrating the steady Navier-Stokes equations over a control volume and transforming this volume integral into a surface integral by using Gauss theorem, the following equation is obtained;

$$F_i = \iint_{\Gamma} \left(u_i u_j n_j + p n_i \delta_{ij} - \frac{1}{\mathrm{Re}}\left(\frac{\partial u_i}{\partial x_j} + \frac{\partial u_j}{\partial x_i}\right) n_j \right) d\Gamma + \iiint_{\Omega} \frac{\partial u_i}{\partial t} d\Omega \tag{8}$$

where Γ is the surface of a control volume and n is the unit vector normal to the surface. By using equation (8), the forces acting on an object are computed. This hydrodynamic force, F_i, is then used together with the gravitational force, G, to solve for the particle velocity using equation (9).

$$F_i - G_i = m_p \frac{dU_i}{dt} \tag{9}$$

SET-UP

The dimensions of the computational domain are 16 x 16 x 32 D with a wall present normal to the x-direction, using a coordinate system as shown in Figure 1. The spheres have a diameter D and a grid resolution of h = D / 16 is used by locally refining a Cartesian grid. The amount of node points is approximately 1000000. A temporal resolution with a CFL number of 0.2 is used for all cases. On all domain boundaries, no slip condition will be applied.

Simulations for a single sphere are performed for different density ratios, viscosities of the fluid and initial position of the sphere. The density ration used are 1.43, 1.5, 2.6, 5, 6.5 and 8. The fluid viscosity is set using a Reynolds number based on the sphere diameter and characteristic velocity set to unity. This Reynolds number is set to 1, 10, 100, 500 and 1000 in the simulations. The sphere is released at four different wall normal distances: 1.5, 3, 4.5 and 6 D.

In dual sphere side-by-side arrangement, one sphere is placed 3 D from the wall with the distance to the centre of the second sphere varying between 1.5, 3, 4.5 and 6 D.

RESULTS AND DISCUSSION

The main focus has been to study particle-wall interaction as well as particle-particle interactions. For all simulations, a grid resolution of 16 cells per sphere diameter was used. The computation of Stokes flow by VOS shows good agreement with the analytical solution and simulations performed by Revstedt (2004).

4.1 Single Sphere

The main forces differentiating a particle falling close to a wall compared to in the middle of a domain are the Saffman force and the Magnus effect. The former are forces due to velocity gradients induced by the wall forcing the sphere to move upward and the latter is due to rotation forcing the particle to move towards the wall. Both these effects induce a lift force. Figure 3 shows the velocity vector field, displaying the non-stationary wake behind the sphere, as a sphere with the density ratio 6.5 is falling three diameters from the wall at Re = 100.

Figures 4 – 6 show the wall normal position of the sphere as a function of time varying the density ratio (Figure 4), the initial position (Figure 5 and 6). For a highly viscous fluid the sphere will tend monotonically towards the wall, but as the Reynolds number is increased the sphere will start to oscillate. The same effect in seen in Figure 4. a low density ratio leads to a low local Reynolds number ($Re_L = U(t)D/\nu$) and a stable path of the sphere. However, as the density ratio is increased so is Re_L and one again observes an oscillatory motion. The effect of the initial distance to the walls is clearly seen in Figure 5 and 6. For low Re (Re = 10), the effect of the wall is decreased with increasing initial wall distance. For Re = 500, one sees no real difference in the oscillation amplitude caused by the presence of the wall. Note though, that at x_0 = 1.5 D, the sphere is initially repelled by the wall while in the other cases the wall attracts the sphere, hence the phase shift in oscillations seen in Figure 6.

Figures 7 and 8 show the solid particle path projected on the x- y plane for density ratio of 6.5 at 3 diameters from the wall for Reynolds numbers 10 and 100, respectively. In the low Reynolds number case the sphere moves in a spiral path as it falls, whereas for Re = 100, the movement is no longer symmetric and the oscillation amplitude is less direction dependent.

Figure 9 depicts the terminal velocity for a Reynolds number of 10 for all density ratios considered. As the Reynolds number is increased and the wake looses its symmetry and becomes unsteady, the terminal velocity is oscillating and the sphere is accelerating faster, this was also observed by Mordant & Pinton (2000). However, the terminal velocity does not appear to be influenced by the distance to the wall.

The oscillations frequency is similar for both velocity components perpendicular to the main direction of motion, and does not seem to be affected by density ratios or Reynolds number. It should be mentioned that for low-density and low Reynolds numbers the velocity components perpendicular to the main flow direction are insignificant and it is therefore difficult to detect any oscillations in these velocity components.

Figure 10 shows the Strouhal number based on the terminal velocity versus the density ratio for Reynolds numbers 10, 100 and 500 for a sphere initially placed three diameters from the wall. For low-density ratios there is a stronger influence on the Strouhal number. The lift force shows similar behavior as the velocity displayed. Independently of distance to the wall, density and the Reynolds number, there is a dominant frequency for the variations of lift force. However, it should be mentioned that the amplitudes of the lift is on the other hand depending on the Reynolds number, density ratio and distance to wall. Close to the wall, an increase in Reynolds number will increase the lift force. Increasing the initial wall distance or decreasing the density ratio results in a decrease of the amplitude of the lift.

4.2 Dual Spheres

Dual spheres falling side by side where the first sphere is placed three diameters from the wall and the second sphere placed 1.5 – 6 diameters from the first sphere was investigated for density ratios 1.5 and 5 at a Reynolds number of 10. Figure 11 displays the velocity field for two spheres with a density ratio of 5 placed 1.5 diameters apart.

For this case, the spheres fall at the same speed, and due to rotation, the spheres first repel each other increasing the separation distance, and then changes direction and move back towards each other again. This periodic motion continues while the spheres settle with an increasing mean separation distance. As the distance between the spheres is increased, the level of interaction between the two particles decreases.

Considering spheres with a density ratio of 5 and placed 1.5 diameters apart, one can observe that dual spheres settling side by side, close to a wall, fall at a lower velocity compared to a single sphere placed at the same distance from the wall. However, Jayaweera *et al* (1963) and Wu & Manasseh (1998) observed experimentally that decreasing the initial distance between the spheres enhanced the falling velocity compared to a single sphere case. This implies that the wall has a strong decelerating effect. This is probably due to a stronger repelling motion in the presence of the wall leading to a larger sphere distance than in the non-wall case, reported by Wu & Manasseh (1998)

The effect of the wall is also visible when studying the motion perpendicular to the wall, Figure 12. The particle closest to the wall seems to be moved out from the wall for a higher density ratio and dragged closer to the wall if the density ratio is low. And, similar to the single sphere case, the motion for the higher density particles is oscillatory. However, the two particles move in opposite direction in relation to each other due to an inward rotation, also detected by Jayaweera et. *al* (1963) and Wu & Manasseh (1998). Considering Figure 13, the movement of dual particles differs significantly from that of a single falling particle. Compared to the dual spheres, a single sphere deviates less from the initial position in the wall normal direction, as is expected.

In the case of a single sphere, the dominant frequency of the motion in the x – and y-directions was detected. Similarly, a frequency was found for the dual sphere cases at higher density ratios. The corresponding Strouhal number is 0.091 for both particles when placed 1.5 diameters apart, and 0.085 when increasing the distance between the particles for a density ratio of 5 and Reynolds number of 10. This can be compared to a Strouhal number of 0.087 obtained for a single particle placed 3 diameters from the wall with the same density ratio and Reynolds number.

CONCLUSIONS

The flow around single and dual spheres falling side by side due to gravity close to a wall have been considered. The presence of the wall will affect the path of the sphere, either attracting or repelling it. The results also showed that the path for a single sphere is highly dependent on the density ratio, Reynolds number and the distance to the wall. In the case of two spherical particles falling side-by-side close to the wall, the effects of interaction between the spheres is stronger than the influence from the wall.

ACKNOWLEDGMENTS

The authors gratefully acknowledge the financial support by the Swedish Research Council. The support of the Centre for scientific computing at Lund University, LUNARC, and the computational resources allocated through SNAC are also gratefully acknowledged.

REFERENCES

Chen, R. C. and Wu, J. L., 2000, "The flow characteristics between two interactive spheres", Chem. Eng. Sci., Vol. 55, pp. 1143-1158.

Folkersma, R., Stein, H. N. and van de Vosse, F. N., 2000, "Hydrodynamic interactions between two identical spheres held fixed side by side against a uniform stream directed perpendicular to the line connecting the spheres' centers", Int. J. Multiphase Flow, Vol. 26, pp. 877-887.

Jayaweera, K. and Manson, B., 1964, "The behavior of clusters of spheres falling in a viscous fluid. Part 1", J. Fluid Mech., Vol. 20, pp. 121-128.

Liang, S.-C., Hong, T. and Fan, L.-S., 1996, "Effects of particle arrangements on the drag force of a particle in the intermediate flow regime", Int. J. Multiphase Flow, Vol. 22 (2), pp. 285–306

Lörstad, D. and L. Fuchs, 2001, "A volume of fluid (vof) method for handling solid objects using fixed Cartesian grids", In B. Sarler and C. A. Brebbia, editors, Moving Boundaries VI – Computational Modelling of Free and Moving Boundary Problems, Wessex Institute of Technology, WIT Press, UK, pp. 143-152.

Mordant, N. and Pinton, J., 2000, "Velocity measurement of a settling sphere", Eur. Phys. J. B, Vol. 18, pp. 343-352.

Olsson P., and Fuchs L., 1998, "The interaction of spherical particles in a fluid flow governed by Navier-Stokes Equations", Proceedings, ECCOMAS, CFD in Multiphase Flows 1, pp. 180-185.

Revstedt, J., 2004, "A virtual Boundary method with improved computational efficiency using a multi-grid method", Int. J. Numer. Meth. Fluids Vol. 45, pp. 775-795.

Tsuji, T., Narutomi, R., Yokomine, T., Ebara, S. and Shimizu, A., 2003, "Unsteady three-dimensional simulation of interactions between flow and two particles", Int. J. Multiphase Flow, Vol. 29, pp. 1431 – 1450.

Wu, J. and Manasseh , R., 1998, "Dynamics of dual-particles settling under gravity", Int. J. Multiphase Flow, Vol. 24, pp. 1343-1358.

Zhao, Y. and Davis, H., 2002, "Interaction of two touching spheres in a viscous fluid" Chem. Eng. Sci., Vol. 57, pp. 1997-2006.

Zhu, C., Lam, K., Chu, H.-H., Tang, X.-D. and Liu, G., 2003, "Drag forces of interacting spheres in power-law fluids", Mech. Research Commun., Vol. 30, pp. 651 – 662.

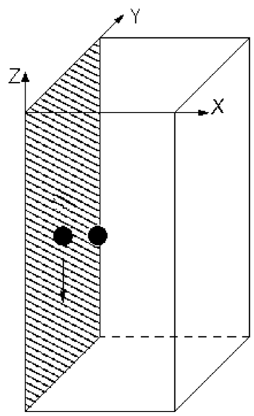

Figure 1. Computational domain

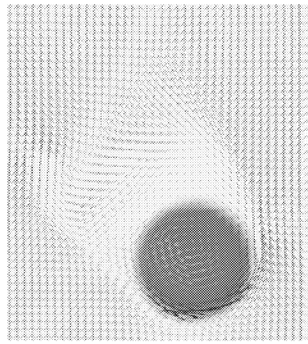

Figure 3. Velocity vector field for a sphere with density ratio of 6.4 at Re = 100 initially placed 3 D from the wall

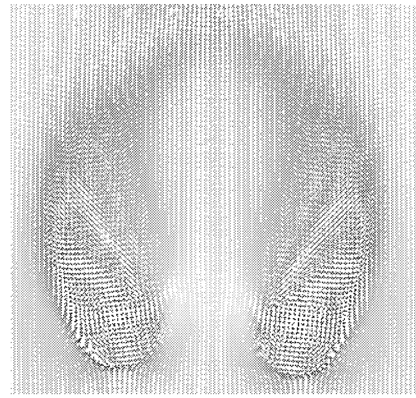

Figure 11. Velocity vector field for dual spheres falling side by side with density ratio of 5 at Re = 10 initially placed 1.5 D apart.

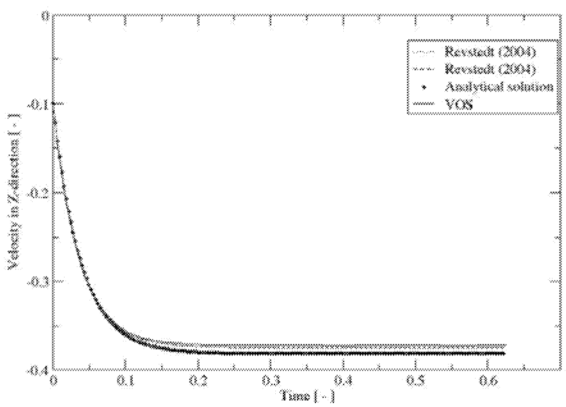

Figure 2. Computation of Stokes flow by VOS compared to the analytical solution and simulations performed by Revstedt (2004)

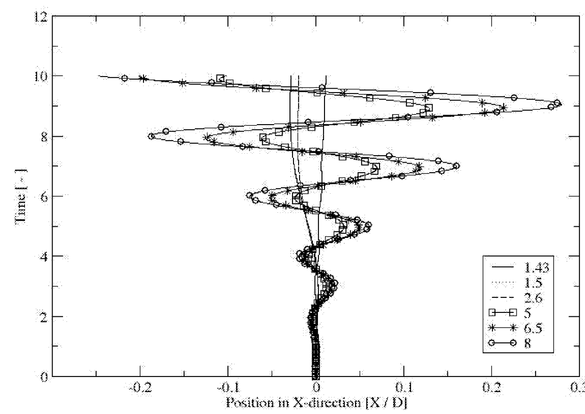

Figure 4. Position in x-direction for different density ratios for a single sphere at Re = 100, wall at – 3D

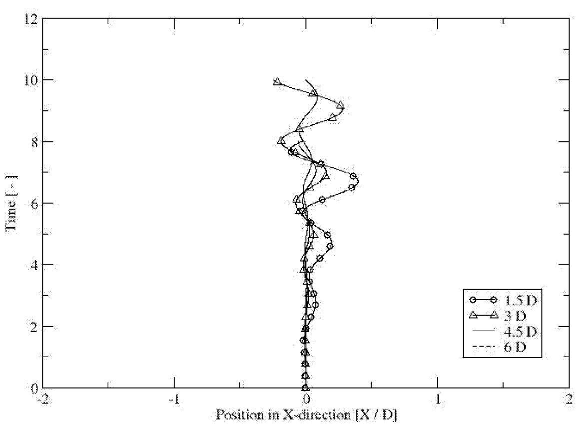

Figure 5. Position in x-direction for different initial positions for a single sphere with density ratio of 8 at Re = 10. The x-axis shows the relative position around the initial position.

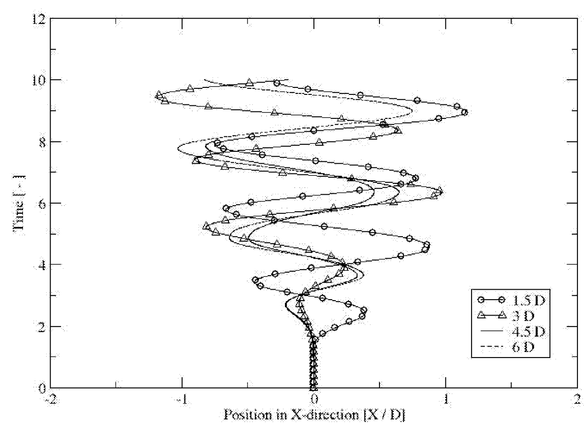

Figure 6. Position in x-direction for different initial positions for a single sphere with density ratio of 8 at Re = 500. The x-axis shows the relative position around the initial position.

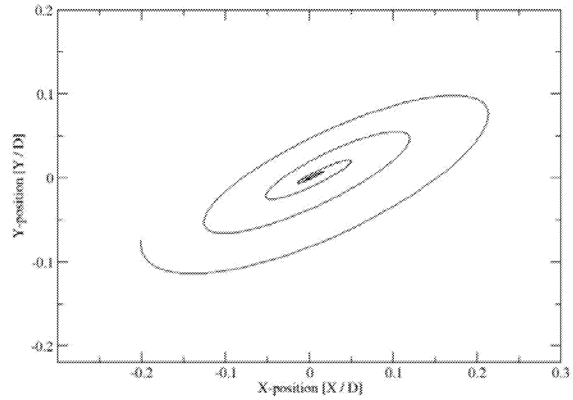

Figure 7. The path of a solid particle projected on the x- y plane for density ratio of 6.5 at 3 diameters from the wall for Reynolds numbers 10.

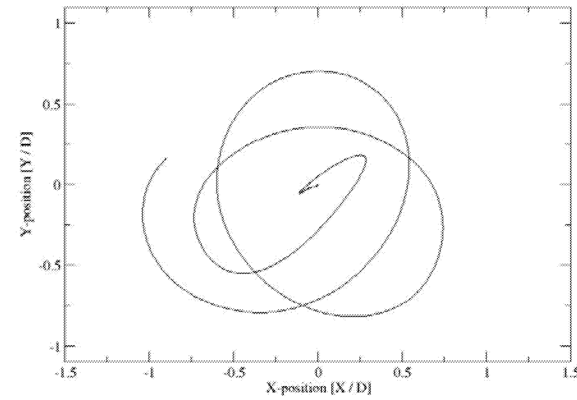

Figure 8. The path of a solid particle projected on the x- y plane for density ratio of 6.5 at 3 diameters from the wall for Reynolds numbers 100.

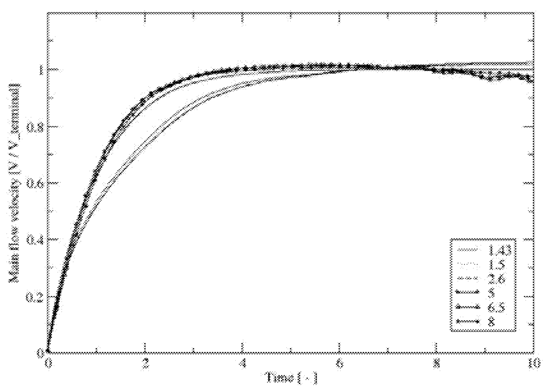

Figure 9. The terminal velocity for a Reynolds number of 10 for all density ratios

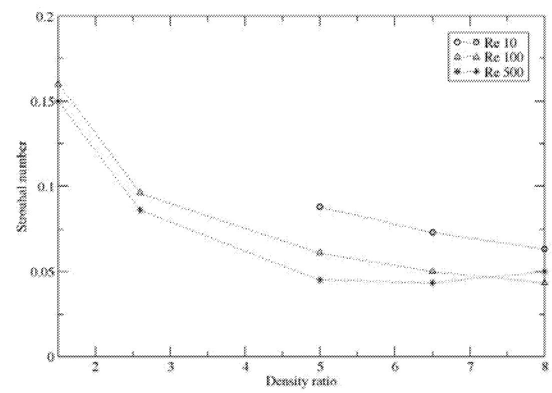

Figure 10. The Strouhal number based on the terminal velocity versus the density ratio for Reynolds numbers 10, 100 and 500 for a sphere initially placed 3 diameters from the wall

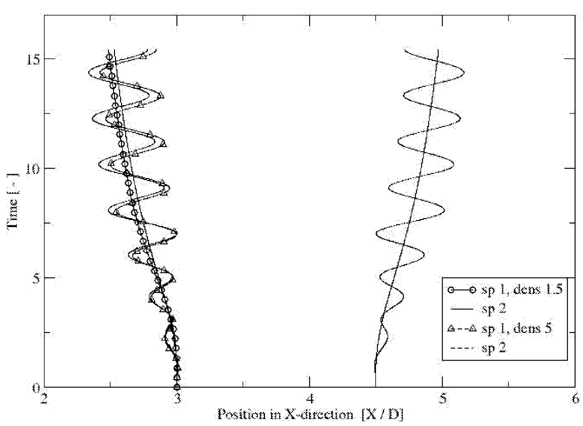

Figure 12. Position of dual spheres falling side by side for an initial separation distance of 1.5 D at Re = 10. On the L.H.S., the position of the second sphere is projected to the path of the first sphere. Wall is at located at "0".

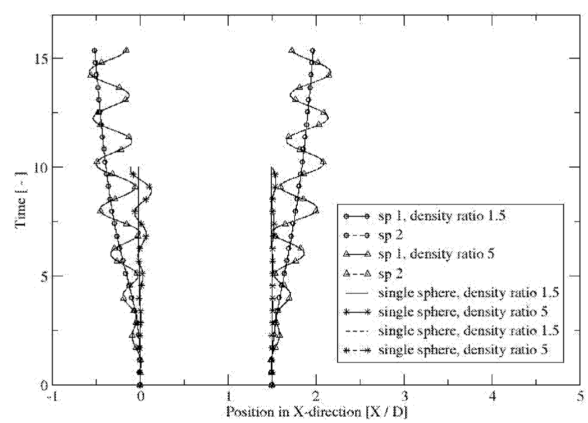

Figure 13. Position of dual spheres falling side by side for an initial separation distance of 1.5 D at Re = 10. On the L.H.S., the position of the second sphere is projected to the path of the first sphere. Wall is at located at "0". Also, the path of a single sphere placed at 3 D and 4.5 D from the wall are displayed.